Accuracy Improvement of a Multi-MEMS Inertial Measurement Unit by Using an Iterative UFIR Filter

Raouf Rasoulzadeh
Department of Electrical, Biomedical and Mechatronics Engineering
Qazvin branch Azad Islamic University
r.rasoulzadeh@qiau.ac.ir

Alireza Mohammad Shahri
Department of Electrical, Biomedical and Mechatronics Engineering
Qazvin branch Azad Islamic University
shahri@iust.ac.ir

Abstract— **In this paper a two layers multi-sensor fusion method is presented to combine output of four low cost, low accuracy MEMS inertial measurement units (IMU) to be used in an inertial navigation system (INS). A Minimum Mean-Square-Error (MMSE) criterion measurement fuser in the first and an iterative unbiased finite impulse response filter in the second layer are utilized to reduce measurement noise effect. The static experimental results verify that angle random walk (ARW) error for x,y and z axes of combined gyroscope reduces up to 2.37 times. Moreover dynamic experimental results show that by choosing optimal horizon interval, the standard deviation of the multi-IMU decreases by a factor of 5 respect to the mean standard deviation of the four sensors that leads to accuracy improvement compared to the single sensor.**

Keywords— IMU; multi-sensor fusion; Iterative UFIR filter; Inertial Navigation System

I. INTRODUCTION

Inertial Measurement Unit, containing gyroscope and accelerometer is the most important component in inertial navigation systems (INS) that are used to obtain orientation, velocity and position of a vehicle. Since the main disadvantage of Micro-Electro-Mechanical-Systems (MEMS) based inertial sensors is their low accuracy of output signal, it is essential to study in more details about the model and types of errors. The inertial sensor errors consist of deterministic and stochastic error types. The deterministic errors includes constant biases, scale factors and misalignment, which are removed from raw measurements by calibration procedures.

The stochastic errors contain random errors (noises) such as angle random walk (ARW), bias instability and rate random walk (RRW) for gyroscope, which cannot be removed from the measurements and should be considered as stochastic models. These types of errors also make significant drift in velocity and position that obtain by accelerometer. Since MEMS IMUs are low cost, small size with low power consumption, it is quite easy to implement a few of them in a small electronic circuit board. Hence, many research studies has been performed to reduce stochastic errors and improve the accuracy by applying multiple MEMS IMUs and combining their output signals. In [1] Bayard and Ploen initially have introduced a virtual gyroscope and designed an optimal Kalman filter to combine output signals of multiple gyros. Bayard has shown the existence of noise correlation between the individual sensors will improve about 170 times the accuracy of the virtual gyroscope. Chang et al [2]-[5] have implemented a hardware with six gyroscopes and applied the Bayard optimal Kalman filter as a simulation and experimental method to estimate angular rate. Consequently, worthy dynamic performance of the Kalman filter with two different stochastic models are shown in theses researches. In [6] some cheap gyroscopes and accelerometers are used to design a low cost IMU array but stochastic modeling for this system are not considered and simply the static test is performed for the assembled hardware. Tanenhaus [7] has also implemented a hardware containing two DSP processors and 100 MEMS inertial sensors for a UAV aiming to fly in the GPS denied environment. In this work the measurement of the sensors are fused by a sigma-point Kalman filter and the performance of the hardware is nearly equal to a fiber optic inertial sensors. Skog and et al [8] have implemented a Multi-IMU platform with 18 cheap IMUs for pedestrian navigation while a simple averaging method is used to reduce stochastic errors. In [9] a multi-IMU hardware is implemented with four sensors by recursive Kalman filter. The performance of the hardware is investigated using static experiment. In [10] the performance of two Kalman filter schemes based on the direct and differencing estimated model of a virtual gyroscope is also analyzed. Results show that the performance of the direct estimated model is much higher compare to the differencing model with a constant input rate signal.

Most of the research studies have been performed based on the Kalman filtering approach. After decades' developments, the finite impulse response (FIR) filter has become a strong competitor to the infinite impulse response filters, including the Kalman filter (KF). Some fundamental works can be found in [11]–[14], which show that the FIR-type filters have some useful properties, such as robustness against temporary modeling uncertainties, bounded input/bounded output stability, low sensitivity to inaccurate noise statistics,. Among them, a distinctive one is the unbiased FIR (UFIR) filter developed in [15], which allows us to ignore the noise statistics and initial states with an optimal estimation horizon.

In this paper, we propose to use a MMSE criterion fuser with an iterative unbiased finite impulse response filter in the multi-IMU application to provide more accurate angular rate while computational complexity is reduced significantly. The rest of this paper proceeds as follows. In section 2 the theoretical operation of the implemented Multi-IMU will be introduced and noise coefficients obtain experimentally. In section 3 the implemented hardware will be explained in more details. In section 4 the gyroscope results of static and dynamic experiments will be presented to show and verify the aim of this research.

978-1-5090-5922-5/17/$31.00 ©2017 IEEE

II. METHODOLOGY

A. Measurement and State-Space Model

The output of the inertial sensors are normally corrupted by some deterministic and stochastic errors such as measurement noise, deterministic bias and bias drift. A general model for the gyroscope could be defined as [16]:

$$y = \omega + b_d + b_r + v \tag{1}$$

Where y is the measured angular rate, ω is the true angular rate, b_d is the deterministic bias or offset of the sensor which can be calculated by long term experiment while the sensor is motionless, b_r is random bias drift which is the bias of the sensor that varies slowly and randomly in time and v is the measurement white noise which causes angle random walk (ARW) error. ARW error is a high frequency noise which is detected in short time that makes an angle drift because of integration from the rate signal measured by sensor. The bias drift term is also the dominant error when the sensor operates for a long time [17].

In this paper, bias drift error can be ignored for short time application, so (1) can be simplified as:

$$y = \omega + v \tag{2}$$

In order to define a state-space model, the next step is to determine dynamic behavior of the sensor. As this sensory system is designed to be utilized in any application, a random walk process that is a typical model for gyroscope behavior is chosen as follows:

$$\omega_{k+1} = \omega_k + w_k \tag{3}$$

By considering (2) and (3) the state-space model for single gyroscope obtains as follows:

$$\begin{cases} x_{k+1} = Fx_k + Gw_k \\ Z_k = Hx_k + v_k \end{cases} \tag{4}$$

Where w_k is process and v_k is measurement noise with the following characteristics:

$$Q = E\left\{w_k . w_k^{\,T}\right\} \quad , \quad R = E\left\{v_k . v_k^{\,T}\right\} \tag{5}$$

Which Q and R are process and measurement noise covariance matrices.

The state-space of multi-IMU with four sensors for single axis estimation are described as:

$$x_k = \omega \, , \quad F = 1 \, , \quad G = T_s \tag{6}$$

$$Z = \begin{bmatrix} y_1 \\ y_2 \\ y_3 \\ y_4 \end{bmatrix} \, , \; H = \begin{bmatrix} 1 \\ 1 \\ 1 \\ 1 \end{bmatrix} \, , \; V = \begin{bmatrix} v_1 \\ v_2 \\ v_3 \\ v_4 \end{bmatrix} \tag{7}$$

where T_s is the sampling time.

B. Multi-Sensor Fusion Algorithm

In this paper a two layers homogenous Multi-Sensor fusion algorithm is proposed. Homogenous term here is used for fusing of identical sensors. At the first layer a minimum-mean-square error criterion fuser and in the second layer an *iterative unbiased finite impulse response* filter were used.

1) Minimum Mean- Square- Error Fuser

The first layer of the Multi-Sensor data fusion algorithm is a measurement fuser which measurement vectors, measurement matrices and measurement noise covariance matrices are combined by using a Minimum-Mean-Square Error criterion. As this multi-sensory system should be used in inertial navigation system (INS) so roll, pitch and yaw angles should be estimated by four sensors. It means the measurement matrix in state-space model contains 12 vectors. By using the first layer fuser it is possible to decrease the dimension of the measurement matrix by a factor of 4. In this layer measurement noise covariance matrices, measurement vectors and measurement matrices obtained from all sensors are combined as follows [18]:

$$R_t = \left[\sum_{i}^{N_s} R_i^{-1} \right]^{-1} \tag{8}$$

$$Z_t = R_t \sum_{i=1}^{N_s} R_i^{-1} y_i \tag{9}$$

$$H_t = R_t \sum_{i=1}^{N_s} R_i^{-1} H_i \tag{10}$$

Where R_t , Z_t and H_t are equivalent measurement noise covariance matrix, measurement vector and measurement matrix respectively.

By considering (8) to (10) the state-space parameters for 3 axes rate estimation changes as follows:

$$x = \begin{bmatrix} \omega_x \\ \omega_y \\ \omega_z \end{bmatrix} \quad , \quad F = I_{3\times 3} \tag{11}$$

$$Z = \begin{bmatrix} z_{t\omega x} \\ z_{t\omega y} \\ z_{t\omega y} \end{bmatrix} \, , \; H = \begin{bmatrix} 1 & 1 & 1 \end{bmatrix}^T \tag{12}$$

2) Iterative Unbised FIR FilterAlgorithm

In many research studies such as [1]-[6] Kalman filtering is most dominant algorithm to fuse sensor measurements of the multi-IMU. In Kalman filter, process and measurement noise covariance matrices should be identified specifically process noise covariance matrix that is usually difficult to find for engineers. In addition Gaussian distribution of the

measurement noise and whiteness are other constraints for KF. These parameters are essential for Kalman filter and the performance of the filter is highly sensitive to these statistics.

In this section an iterative UFIR filter is used after measurement fuser to increase the accuracy of the Multi-Sensor system that yields by decreasing standard deviation of the output rate signal. As UFIR filter ignores noise statistics, it can be optimal for our application as like as any practical application.

Generally UFIR filter is used as batch form and all computations can be performed offline. By considering state-space parameters in (11) and (12), the batch form of the UFIR estimator represented as [19]:

$$\hat{x}_{k|k} = K_N Z_{k,m} \tag{13}$$

Where $Z_{k,m} = \begin{bmatrix} z_k^T & z_{k-1}^T & \dots & z_m^T \end{bmatrix}^T$ is the measurement vector with measurement collected from $m = k - N + 1$ to k, N is horizon interval and K_N is filter gain that computed as:

$$K_N = F^{N-1}(H_{N-1}^T H_{N-1})^{-1} H_{N-1}^T \tag{14}$$

The extended matrices are also defined as follows:

$$F_i = \begin{bmatrix} (F^i)^T & (F^{i-1})^T & \dots & F^T & I \end{bmatrix}^T \tag{15}$$

$$H_i = \overline{H}_i F_i \tag{16}$$

Where $\overline{H}_i$ is $i+1$ dimensional diagonal matrix with elements of H.

It is obvious that computational burden will increase by choosing large value of N when the filter is used in batch form. For this reason an iterative UFIR filter is used for fast computation. In this case it should be defined a matrix, G called *Generalized Noise Power Gain* that is similar to estimation error covariance, P in Kalman filter. This parameter can be used to perceive how much noise will be suppressed at the output of the UFIR estimator [19]. This Matrix can be computed readily by extended matrices from the batch form filter as:

$$G(N) = F^{N-1}(H_{N-1}^T H_{N-1})^{-1}(F^{N-1})^T \tag{17}$$

In this research the proposed Iterative UFIR filter by using an iterative variable, l which implemented in MATLAB software to estimate true angular rate, can be represented as follows:

$$\hat{x}_{l|l-1} = F\hat{x}_{l-1} \tag{18}$$

$$G_{l|l-1} = F_l G_{l-1} F_l^T \tag{19}$$

$$G_l = \begin{bmatrix} H_l^T H_l + (F_l G_{l-1} F_l^T)^{-1} \end{bmatrix}^{-1} \tag{20}$$

$$K_l = G_l H_l^T \tag{21}$$

Where $l = k - N + m + 1$ to k and the estimate of the current state is taken when $l = k$. The initial value $\hat{x}_{l-1}$ is computed as in [19].

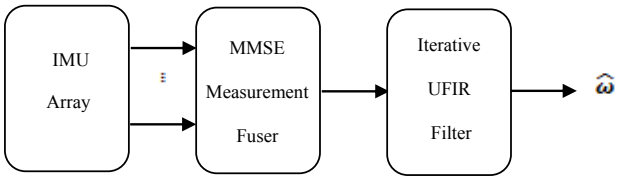

Fig.1. Illustration of the proposed two layers multi-sensor fusion algorithm

As seen two important parameters, Q and R are ignored by UFIR estimator that means the proposed UFIR filter is not sensitive to noise statistics and is also more robust compare to KF. However for this estimator number of optimal horizon interval, N_{opt} should be defined so that estimation error becomes minimum, but this parameter can be determined readily compare to process noise covariance matrix, Q. In Fig 1 a block diagram of the two layers multi-sensor fusion is shown.

C. *Allan Variance Analysis*

In this section the Allan variance method will be introduced to obtain required information about stochastic errors and different noise terms in the original data set. The Allan variance technique is a time domain method which was developed in the mid-1960 for frequency stability of precision oscillators [20] but is commonly used for analyzing inertial sensors. For measured data from inertial sensors assume the output of the sensor is $\Omega(t)$ and the number of data points in each cluster is *n,* the cluster average defined as [17]:

$$\overline{\Omega}_k(T) = \frac{1}{T}\int_{t_k}^{t_k+T} \Omega_k(T)dt \tag{23}$$

The Allan variance of a dataset with length T is defined as:

$$\sigma_A^2(T) = \frac{1}{2(N-2n)} \sum_{k=1}^{N-2n} \left[\overline{\Omega}_{k+n}(T) - \overline{\Omega}_k(T) \right]^2 \tag{24}$$

After calculating the Allan variance, the next step is to use the root Allan variance plot to identify the magnitude and type of the noise that exists in the data. It is normally plotted as the square root of the Allan variance $\sigma_A(T)$ versus T on a logarithmic scale. In Fig 2 a plot of the Allan variance curve obtained from a single sensor is shown as an example. By using this curve it is possible to identify noise terms in the signal by investigating different slope lines. A pure white noise model which is a wideband noise and is detected in short time appears in a root Allan variance curve as a line with -1/2 slope which causes ARW error in the inertial sensor. The random bias drift (RRW) error which is detected in long time is a band limited frequency noise which is identified by a line with slope +1/2.

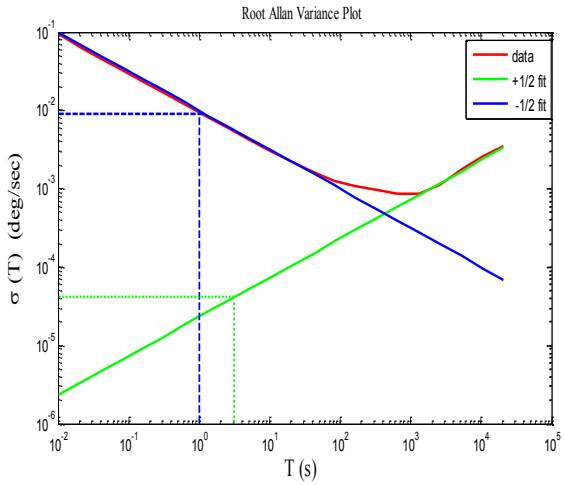

Fig.2. Root Allan variance of a single sensor with different slope lines which detrmines ARW and RRW at $T=1$ and $T=3$.

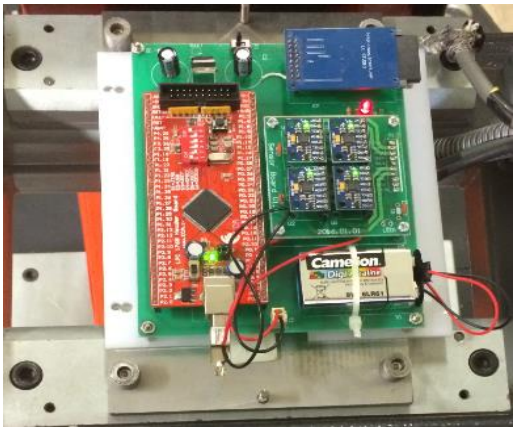

Fig.3. Implemented gyroscope array containing 4 MPU9150 modules from InvenSense, LPC1768 Cortex microcontroller from NXP and a SD card in order to collect data.

Thus for computing ARW and RRW coefficient for each sensor a line with -1/2 and +1/2 slope fitted to the curve and the value of $\sigma_A(T)$ computed at $T=1$ and $T=3$ by [17]:

$$\sigma_A^2(T)=\frac{ARW^2}{T} \tag{25}$$

$$\sigma_A^2(T)=\frac{RRW^2T}{3} \tag{26}$$

In this research a static long term experiment was conducted with implemented hardware and experimental data gathered from all sensors to identify stochastic errors. Duration of the test is 24 hours with 100 Hz sampling frequency which ARW and RRW coefficients obtain as in TABLE 1. As seen the RRW error is too small so the assumption of ignoring random bias drift in (2) can be correct. In this paper measurement noise variance of the measurement vector, R_i which is used in (8) - (10) is formed by square of ARW coefficients from TABLE 1. The deterministic bias or offset of the sensor can also be calculated from the mean value of the static data and subtracted from the measurement in the actual condition.

III. HARDWARE IMPLEMENTATION

To verify the proposed algorithm a hardware is designed and consequently implemented applying of four MPU9150 IMU sensors made by InvenSense [22]. These four sensors are located somehow to form a planar IMU array as shown in Fig3. The LPC1768 Cortex M3 ARM microcontroller [23] is selected as the main processor of this multi-IMU board.

The important issue of designing this system is to collect the data of four sensors simultaneously in real-time. The I2C protocol is used as the communication method to collect the data of four IMU sensors. As I2C is a 2 wire serial interface, by using an optimal firmware in C programming, the time difference between collecting data of each sensor is less than 0.12 [msec]. In this hardware, General Purpose Input Output (GPIO) of the microcontroller defined as I2C interface so that two GPIOs are used for SCL and SDA to collect measurement data. In this way the limitation on the number of IMUs is defined by the number of available GPIO on the microcontroller. As in dynamic test the hardware rotates continuously it is impossible to send data to the host computer via USB connection therefore a SD Card Module is also used to store the measured data.

IV. RESULTS

A. Constant Rate Experiment

In this section a dynamic test with constant rate rotation was performed to analyze the performance of the multi-sensory system. Constant rate test was carried out by a 3 degree of freedom turn table with calibration capability as shown in Fig 4. The turn table rotates 360 degrees around z-axis and only 70 degrees around x and y so the constant rate test has been peformed for z-measurement of gyroscope. The hardware which contains IMU array is attached to the table tightly. The sampling frequency was set to 200 Hz and measurement range for all gyroscopes set to $2000\,^\circ/s$. The experiment is carried out for $\omega=12,24,42,60,90$ and $150\,^\circ/s$ with duration of 5 minutes.

Table 1. ARW coefficients of 24 hours static test

Sensor	ARW $(^\circ/\sqrt{s})$	RRW $(^\circ/\sqrt{s^3})$	Sensor	ARW $(^\circ/\sqrt{s})$	RRW $(^\circ/\sqrt{s^3})$	Sensor	ARW $(^\circ/\sqrt{s})$	RRW $(^\circ/\sqrt{s^3})$
Gx1	0.0108	3.5716×10^{-5}	Gy1	0.0107	4.4562×10^{-5}	Gz1	0.0126	1.3711×10^{-4}
Gx2	0.0095	6.1214×10^{-5}	Gy2	0.0094	3.2564×10^{-5}	Gz2	0.0087	4.6276×10^{-5}
Gx3	0.0106	1.0281×10^{-5}	Gy3	0.0111	5.6559×10^{-5}	Gz3	0.0100	4.2848×10^{-5}
Gx4	0.0103	4.9936×10^{-5}	Gy4	0.0103	7.1984×10^{-5}	Gz4	0.0108	1.7139×10^{-5}

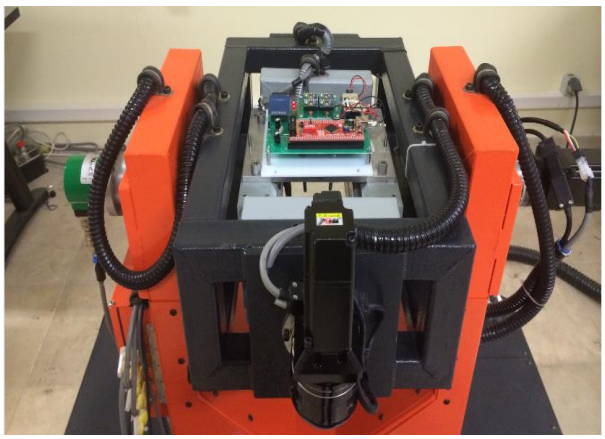

Fig.4. 3-axes turn table was used to conduct dynamic experiment

TABLE 2. Standard deviation of rate signal measured by single gyroscope

Rate $(^\circ/s)$	Gz1 $(^\circ/s)$	Gz2 $(^\circ/s)$	Gz3 $(^\circ/s)$	Gz4 $(^\circ/s)$
$\omega=12$	0.1152	0.0929	0.0936	0.0924
$\omega=24$	0.1243	0.0884	0.0883	0.0874
$\omega=42$	0.3516	0.1352	0.1160	0.1151
$\omega=60$	0.3745	0.1263	0.1314	0.1391
$\omega=90$	0.5602	0.1587	0.1654	0.7089
$\omega=150$	0.6389	0.1923	0.1850	0.1885

At first the results of 1σ error of the measured value by each sensor is shown in TABLE 2. It is clear that however all sensors were chosen from the same manufacturer with the same model but the standard deviation obtained by sensors are not identical, hence the mean standard deviation of four sensors, σ_m can be calculated and used as a reference to compare the results. The results of combined rate signal with different horizontal interval, and calculated σ_m is shown in TABLE 3 that is obvious accuracy improvement with small N is insufficient which by increasing horizontal interval the standard deviation of the combined rate signal reduces compared to σ_m significantly. It needs to be pointed out here the aim of accuracy improvement is to lower the standard deviation of the measurement.

B. Practical approach to Choose N_{opt} for UFIR Filter

For applying UFIR filter to the multi-MEMS application an optimal horizon interval, N_{opt} should be defined. There are some methods to choose optimal horizon interval in [13], [23] and [24] which are based on minimizing generalized noise power gain, but in this research a practical approach is proposed by considering dynamic characteristic of the gyroscope.

As inertial sensor may be objected to the alternating input, reproducing of the input signal should be performed without attenuation.

As the output signal is provided by the multi-sensor fusion algorithm, the performance of the iterative UFIR filter in reproducing of the input signal is investigated by applying a sinusoidal signal with characteristic of 0.5 Hz frequency and $45^\circ/s$ magnitude to the iterative UFIR filter. The results of the filter output are shown in Fig 5 that illustrates attenuation of the output signal grows up slightly by increasing of N that can be taken into account as *scale factor* error for inertial sensor. It means there is a limitation to choose large N_{opt} in this application. Therefore by trading off between the dynamic characteristic of the sensor and obtaining higher accuracy, $N_{opt}=30$ is chosen for the proposed filter. By this value magnitude of the generated signal is $44.58^\circ/s$ which reproduces input signal about 0.95% (less than 1%) However it is possible to get less attenuation by $N=$ 15, 20 and 25 (0.2%, 0.5% and 0.7% attenuation).

According to the TABLE 2 and 3 and by choosing $N_{opt}=30$ for the iterative UFIR filter, accuracy improvement of the multi-IMU in constant rate experiment is nearly 5 times respect to the mean standard deviation obtained from four sensors. Also Fig 6 and 7 illustrate the 5 minutes plots of single sensor measurement and combined rate signal for different angular rates. It is clear by combining multiple sensors the drift of the obtained data from multi-sensory system reduces significantly.

Table 3. Standard deviation of combined rate signal with different horizon interval for dynamic experiment

$\omega(^\circ/s)$	$\sigma(^\circ/s)$ $N=10$	$\sigma(^\circ/s)$ $N=15$	$\sigma(^\circ/s)$ $N=20$	$\sigma(^\circ/s)$ $N=25$	$\sigma(^\circ/s)$ $N=30$	$\sigma(^\circ/s)$ $N=35$	$\sigma(^\circ/s)$ $N=40$	σ_m
$\omega=12$	0.0394	0.0256	0.0224	0.0216	0.0206	0.0175	0.0167	0.0985
$\omega=24$	0.0403	0.0367	0.0329	0.0299	0.0272	0.0249	0.0232	0.0971
$\omega=42$	0.0659	0.0563	0.0478	0.0413	0.0363	0.0326	0.0305	0.1794
$\omega=60$	0.0860	0.0694	0.0557	0.0472	0.0442	0.0431	0.0408	0.1928
$\omega=90$	0.1255	0.0958	0.0834	0.0779	0.0694	0.0613	0.0569	0.3476
$\omega=150$	0.1176	0.1006	0.0821	0.0728	0.0603	0.05	0.0420	0.3011

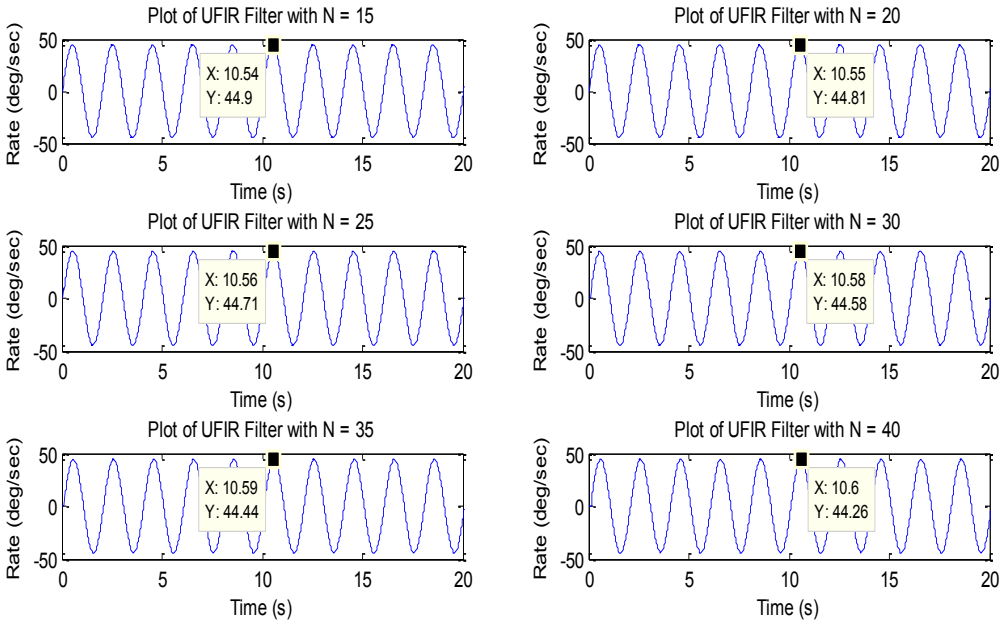

Fig 5. Illustration of periodic signal reproduced by UFIR filter with different horizon interval

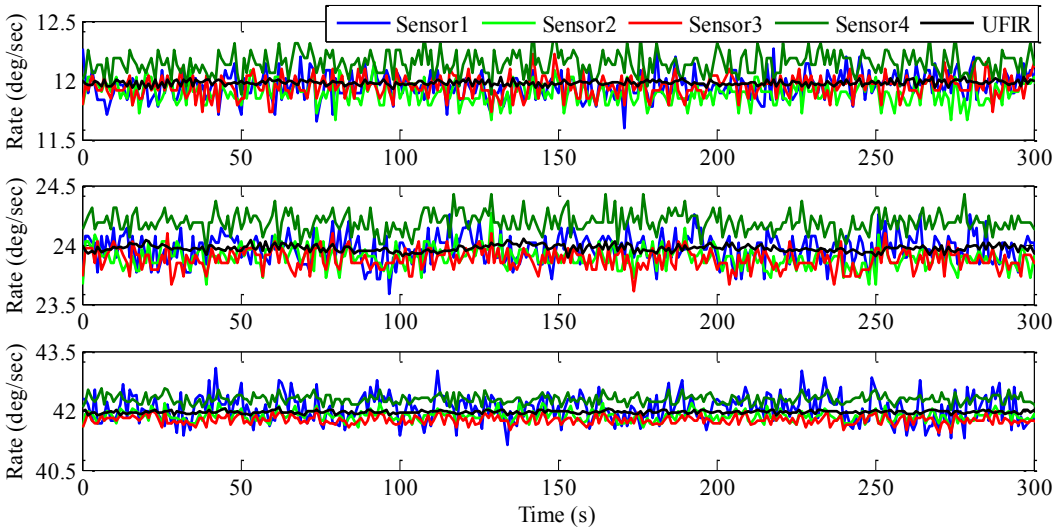

Fig 6. Illustration of the constant rate experiment for $\omega = 12, 24, 42°/s$

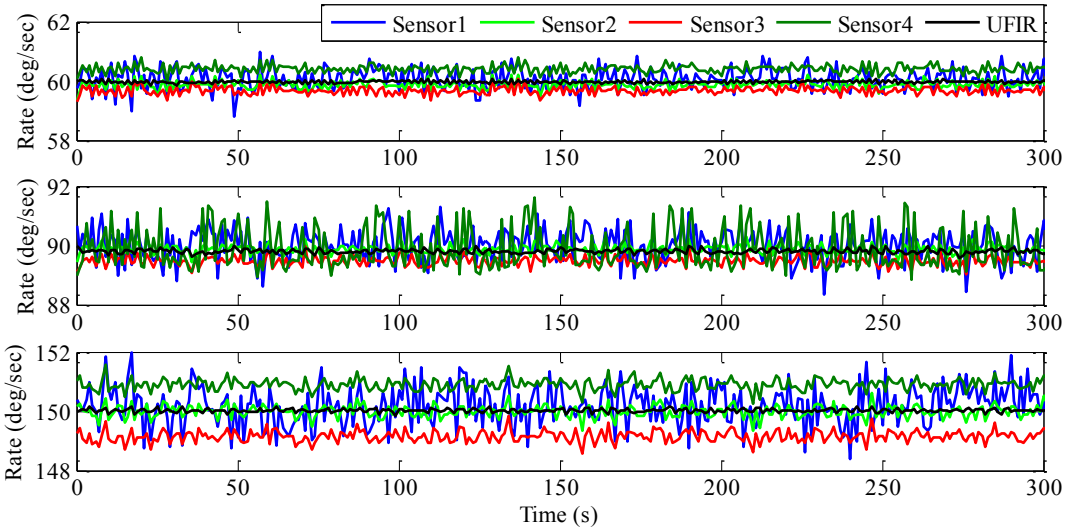

Fig 7. Illustraion of the constant rate experiment for $\omega = 60, 90, 150°/s$

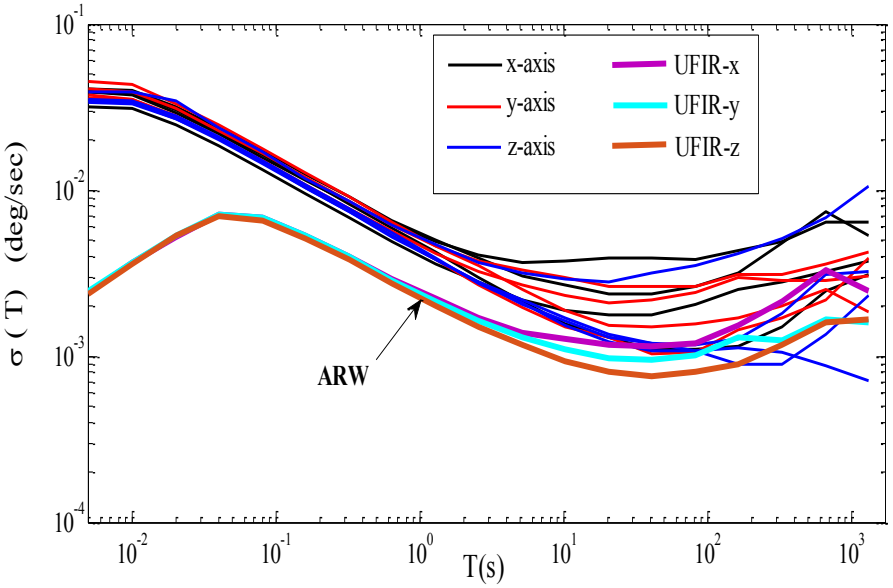

Fig 8. Root Allan variance plot of 2 hours static experiment.

Table 4. ARW coefficients of 2 hours static experiment

Sensor	ARW ($°/\sqrt{s}$)	Improvement Single sensor/UFIR	Sensor	ARW ($°/\sqrt{s}$)	Improvement Single sensor/UFIR	Sensor	ARW ($°/\sqrt{s}$)	Improvement Single sensor/UFIR
Gx1	0.0044	1.83	Gy1	0.0048	2.08	Gz1	0.0053	2.4
Gx2	0.0049	2.04	Gy2	0.0045	1.95	Gz2	0.0045	2.04
Gx3	0.0057	2.37	Gy3	0.0054	2.37	Gz3	0.0044	2
Gx4	0.0055	2.29	Gy4	0.053	2.3	Gz4	0.0046	2.09
UFIR	0.0024		UFIR	0.0023		UFIR	0.0022	

A. Static Performance Analysis

In this section the performance of the system to decrease ARW error will be investigated by a static experiment. A two hours static experiment with $f_s = 200Hz$ and $N_{opt} = 30$ is performed while the hardware is motionless. ARW error coefficient of the combined rate signal is computed for 3-axes of gyroscope and comparative results are shown in TABLE 4 that indicates a reduction of ARW between 1.83-2.4 times compared to the single sensor. If the mean ARW of the four sensors is considered, the noise reduction obtain by a factor of 2.13, 2.17 and 2.13 for x,y and z axes respectively. The root Allan variance plot of static experiment is also shown in Fig 8. To demonstrate the effectiveness of the multi-sensor fusion approach for noise reduction of MEMS IMU, results for some different combinations of the IMUs are presented in TABLE 5. By evaluating the obtained results, it is found that by adding one sensor to the IMU array, ARW coefficient is reduced about 0.004-0.007 $°/\sqrt{s}$ for all axes. Also for the same number of sensors with different combination there is no difference in ARW reduction and just using more sensor can lower this type of error.

Table 5. Results of the ARW coefficient combinations of different sensors

IMU Sensors				ARW (x-axis) ($°/\sqrt{s}$)	ARW (y-axis) ($°/\sqrt{s}$)	ARW (z-axis) ($°/\sqrt{s}$)
1	2			0.0033	0.0032	0.0034
1	2	3		0.0029	0.0028	0.0027
1	3	4		0.0030	0.0029	0.0027
2	3	4		0.0030	0.0029	0.0026
1	2	3	4	0.0024	0.0023	0.0022

V. CONCLUSION

In this paper an IMU array sensor with low accuracy, low-cost sensor is implemented to fuse their measurements in order to increase the accuracy of the sensory system compare to the single sensor. ARW and RRW errors of the MEMS-IMUs were evaluated by 24 hours experimental data and Allan variance technique. A two layers measurement fusion algorithm was employed in the multi-IMU problem to estimate high-accuracy angular rate while computational complexity is reduced significantly. By trading off between the dynamic characteristic of the IMU and obtaining higher

accuracy, a practical approach was represented to choose N_{opt} for proposed filter.

The performance of the implemented hardware and multi-sensor data fusion algorithm was investigated by dynamic and static experiments. The results with $N_{opt} = 30$ show that the accuracy of the hardware in dynamic test improves by a factor of 5 respect to the mean standard deviation of the four sensors and in static analysis performance, one of the major stochastic error, ARW for combined signal reduces to 0.0024, 0.0023 and $0.0022\,^{\circ}/s$ for x,y and z-axes respectively. The results show that by using multiple MEMS sensors instead of a single sensor both ARW and 1σ error in static and dynamic conditions are reduced significantly.

It should be pointed out, however the proposed multi-sensor fusion algorithm have been verified for gyroscope, potentially it could be applied for accuracy improvement of MEMS accelerometer as a future work.

REFERENCES

[1] D. S. Bayard and S. R. Ploen, "High accuracy inertial sensors from inexpensive components," U.S. Patent 0 187 623, Oct. 2, 2003.

[2] H. Chang, L. Xue, W. Qin, G. Yuan and W. Yuan, "An Integrated MEMS Gyroscope Array with Higher Accuracy Output," Sensors ,pp.2886-2899, August 2008.

[3] H.Chang, L.Xue, C.Jiang, M.Kraft, W.Yuan, "Combining numerous uncorrelated MEMS Gyroscopes for Accuracy Improvement Based on

an Optimal Kalman Filter," IEEE Transactions on Instrumentation and Measurement ,vol. 61, pp. 3084-3093, 2012.

[4] C. Jiang,L. Xue,H. Chang,G. Yuan, W.Yuan, Signal processing of MEMS gyroscope arrays to improve accuracy using a 1st order Markov for rate signal modeling. Sensors **2012**, 12, 1720–1737.

[5] L.Xue, L.Wang, T.Xiong, C.Jiang, and W.Yuan," Analysis of Dynamic Performance of a Kalman Filter Combining Multiple MEMS Gyroscope " micromachines 2014,5, 1034–1050.

[6] H. Martin and P. Groves, "A new approach to better low-cost MEMS IMU performance using sensor arrays," in Proc. ION GNSS+, Sept. 2013.

[7] M. Tanenhaus, D. Carhoun, T. Geis, E. Wan, and A. Holland, "Miniature IMU/INS with optimally fused low drift MEMS gyro and accelerometers for application in GPS-denied environments," in Proc. IEEE/ION PLANS, Apr. 2012.

[8] I. Skog, J.-O. Nilsson, and P. Händel, "An open-source multi inertial measurement units MIMU) platform," in Proc. Int. Symp. on Inertial Sensors and Systems (ISISS), (Laguna Beach, CA, USA), Feb. 2014.

[9] R. Rasoulzadeh, A.M.Shahri, "Implementation of A Low-Cost Multi – IMU Hardware by Using a Homogenous Multi-Sensor Fusion" 4th International Conference on Control, Instrumentation and Automation, January 27-28, Qazvin, Iran

[10] G.Yuan , W. Yuan 1, L. Xue , J. Xie and H. Chang " Dynamic Performance Comparison of Two Kalman Filters for Rate Signal Direct Modeling and Differencing Modeling for Combining a MEMS Gyroscope Array to Improve Accuracy" Sensors **2015**, FF15, 27590-27610;

[11] W. H. Kwon, P. S. Kim, and P. Park, "A receding horizon Kalman FIR filter for discrete time-invariant systems," *IEEE Trans. Autom. Control*, vol. 44, no. 9, pp. 1787–1791, Sep. 1999.

[12] W. H. Kwon, P.S. Kim, S. H. Han, "A receding horizon unbiased FIR for discrete-time state space models, " *Automatica*, vol. 38, no. 3, pp. 545-551, Mar. 2002.

[13] Y. S. Shmaliy, "Linear optimal FIR estimation of discrete time-invariant state-space models," *IEEE Trans. Signal Process.*, vol. 58, no. 6, pp. 3086–3096, Jun. 2010.

[14] Y.S.Shmali, "Suboptimal FIR filtering of non-linear models in additive white gaussian noise," *IEEE Transs. Signal Process*., vol. 60, no. 10, pp. 5519-5527, Oct. 2012.

[15] Y.S.Shmali, " An iterative Kalman-Like algorithm ignoring noise and initial conditions, " IEEE Trans. Signal Process., vol. 59, no. 6, pp. 465-2473, Jun 2011.

[16] IEEE Standard Specification Format Guide and Test Procedure for Coriolis Vibratory Gyros no.1, pp. 140–149, Jan. 2008,IEEE Std. 1431, 2004.

[17] N. El-Sheimy, H. Hou, and X. Niu, "Analysis and modeling of inertial sensors using Allan variance," *IEEE Trans. Instrum. Meas.*, vol. 57,

[18] Q.Gan and C.J.Harris, "Comparison of two Measurment Fusion methods for K.Filter Based Multisensor data Fusion" , IEEE Trans on Aerospace and Electronic sys. , vol.37 , No.1 January 2001, 273-280.

[19] Y. S. Shmali and D. Simon, " Iterative unbiased FIR state estimation: A review of algorithms," EURASIP J. Adv. Signal Process., vol. 2013, no. 1, pp. 1-16, 2013.

[20] D. W. Allan, "Statistics of atomic frequency standards," *Proc. IEEE*, vol. 54, no. 2, pp. 221–230, Feb. 1966.

[21] InvenSens MPU9150 Motion Sensor Document number: PS-MPU9150A, Rev4.0

[22] NXP (Phillips), ;LPC17xx 32-bit ARM Cortex-M3 microcontroller, Rev. 5.3

[23] Y. S.Shmali, J. Mu˜noz-Diaz, , L. Arceo-Miquel, "Optimal horizons for a One-parameter family of unbiased FIR filters. Digital Signal Process 18, 739-750 (2008).

[24] F.Ramirez-Echeverria, A Sarr, Y.S Shmaliy, Optimal memory fordiscrete-time FIR filters in state-space. IEEE Trans. Signal Process (2013).